Efficient Polarimetric Analysis of Accretion Disks around Kerr Black Holes

arXiv:2308.15159

Vladislav Loktev (University of Turku)

30.08.2023, Česky Krumlov

South Bohemian X-ray polarisation workshop

IXPE GO proposals for BH XRBs and AGN

belliavesha.github.io

Modeling the polarization spectrum

1. Geometry of the system
2. Local emission at the disk
3. Gravitational redshift and Doppler boosting
4. Light bending and rotation of the polarization frame

Modeling the polarization spectrum

Geometry

- Assume thin equatorial disk
- For a soft state disk around a Kerr BH, the inner radius of the disk depends on the spin parameter

Redshift

- For the emissionfrom from the equatorial plane of the BH, the SR and GR redshift is computed analytically

Local emission

- The radial emission pattern also depends on spin, null hypothesis (and our example) is a standard thin disk described in [Novikov & Thorne (1973)]

- As a simples local atmosphere model we can adopt Chandrasekhar's electron sattering atmosphere.

Insert your analytically described model here.

Modeling the polarization spectrum

Geometry

- Assume thin equatorial disk
- For a soft state disk around a Kerr BH, the inner radius of the disk depends on the spin parameter

Redshift

- For the emissionfrom from the equatorial plane of the BH, the SR and GR redshift is computed analytically

$$r_{\rm ISCO} = \frac{1}{2}\left(3 + Z_2 \pm \sqrt{(3 - Z_1)(3 + Z_1 + 2Z_2)}\right)$$

$$Z_1 = 1 + \sqrt[3]{1 - a^2}\left(\sqrt[3]{1 + a} + \sqrt[3]{1 - a}\right)$$

$$Z_2 = \sqrt{3a^2 + Z_1^2}.$$

Local emission

- The radial emission pattern also depends on spin, null hypothesis (and our example) is a standard thin disk described in [Novikov & Thorne (1973)]

- As a simples local atmosphere model we can adopt Chandrasekhar’s electron sattering atmosphere.

Modeling the polarization spectrum

Geometry

- Assume thin equatorial disk
- For a soft state disk around a Kerr BH, the inner radius of the disk depends on the spin parameter

Redshift

- For the emissionfrom from the equatorial plane of the BH, the SR and GR redshift is computed analytically

Local emission

- The radial emission pattern also depends on spin, null hypothesis (and our example) is a standard thin disk described in [Novikov & Thorne (1973)]

- As a simples local atmosphere model we can adopt Chandrasekhar's electron sattering atmosphere.

$$T_{\rm eff}^4(r) = \frac{3GM\dot{M}}{8\pi\sigma_{\rm SB}R^3} f(r,a) = T_*^4 \frac{f(r,a)}{r^3},$$

$$F_{E'} = \frac{\pi}{f_{\rm col}^4} B_{E'}(f_{\rm col} T_{\rm eff})$$

$$a_{\rm es}(\zeta') = \frac{60}{143}(1 + 2.3\cos\zeta' - 0.3\cos^2\zeta')$$

$$p_{\rm es}(\zeta') = 0.1171 \frac{1-\cos\zeta'}{1+3.582\cos\zeta'}$$

Modeling the polarization spectrum

Geometry

- Assume thin equatorial disk
- For a soft state disk around a Kerr BH, the inner radius of the disk depends on the spin parameter

Redshift

- For the emissionfrom from the equatorial plane of the BH, the SR and GR redshift is computed analytically

$$\beta = \frac{\mathcal{F}}{\mathcal{B}\sqrt{\mathcal{D}}}\sqrt{\frac{1}{2r}}$$

$$g = E/E' = \gamma\left[\mathcal{X} + \mathcal{Y}\beta + (\mathcal{X}\beta + \mathcal{Y})\cos\xi'\right]$$

where

$$\mathcal{X} = \sqrt{\mathcal{D}/\mathcal{A}}, \qquad \mathcal{B} = 1 + \frac{a}{\sqrt{8r^3}},$$

$$\mathcal{Y} = a/\sqrt{4r^4\mathcal{A}}, \qquad \mathcal{D} = 1 - \frac{1}{r} + \frac{a^2}{4r^2},$$

$$\mathcal{A} = 1 + (r+1)\frac{a^2}{4r^3}. \qquad \mathcal{F} = 1 - \frac{a}{\sqrt{2r^3}} + \frac{a^2}{4r^3}.$$

Local emission

- The radial emission pattern also depends on spin, null hypothesis (and our example) is a standard thin disk described in [Novikov & Thorne (1973)]
- As a simples local atmosphere model we can adopt Chandrasekhar’s electron sattering atmosphere.

Model: Light bending (Kerr)

The Kerr metric

$$(g_{ab}) = \begin{pmatrix} 1-\frac{2Mr}{\rho^2} & 0 & 0 & \frac{2Mra\sin^2\theta}{\rho^2} \\ 0 & -\frac{\rho^2}{\Delta} & 0 & 0 \\ 0 & 0 & -\rho^2 & 0 \\ \frac{2Mra\sin^2\theta}{\rho^2} & 0 & 0 & -\sin^2\theta\left(r^2+a^2+\frac{2Mra^2\sin^2\theta}{\rho^2}\right), \end{pmatrix}$$

Solving geodesic equations,

$$\frac{\mathrm{d}u^a(\lambda)}{\mathrm{d}\lambda} = -\Gamma^a_{bc}u^b u^c + f^a$$

Simple!

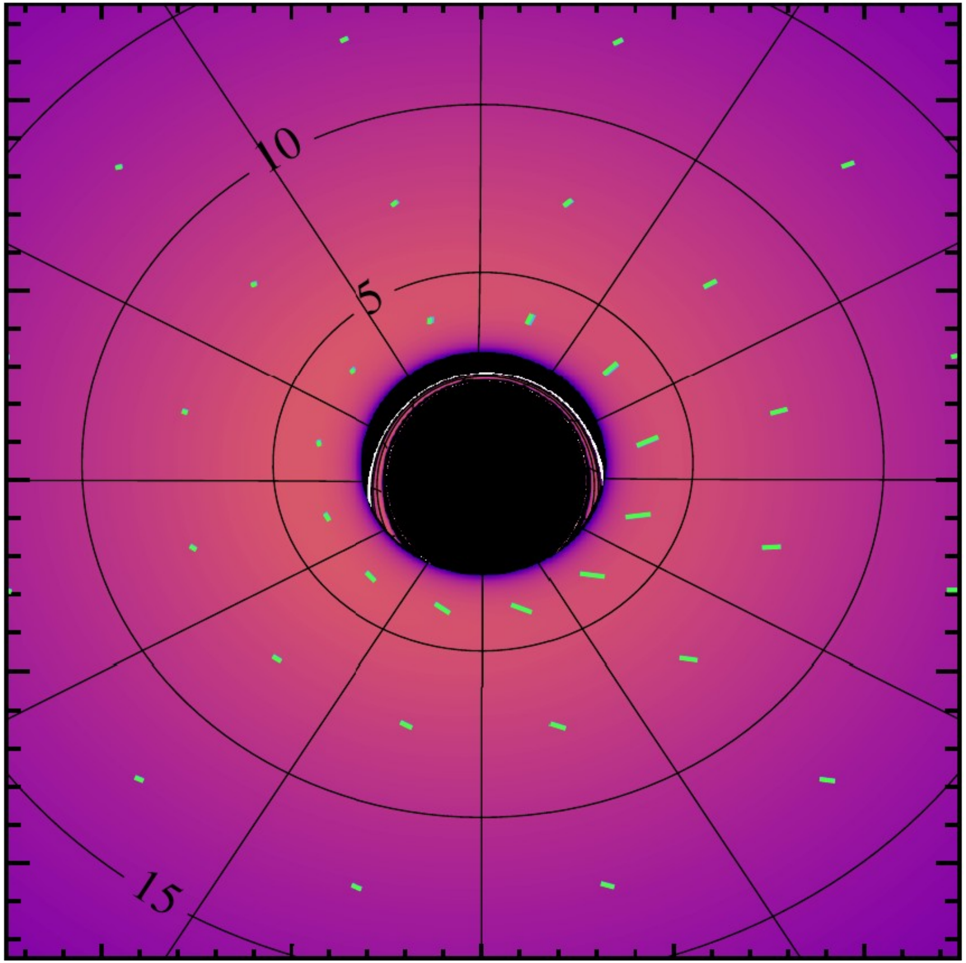

Model: Light bending (Kerr)

$$\frac{\mathrm{d}u^a(\lambda)}{\mathrm{d}\lambda} = -\Gamma^a_{bc} u^b u^c + f^a$$

- We trace the geodesics from the observer **back** to the system
- There are **no analytical** solution to the geodesic equation. (slow)
- The result trajectories in the Kerr metric are **non-planar** due to frame-dragging.
- They are the most different from the zero-spin case at the **very vicinity** to the BH.

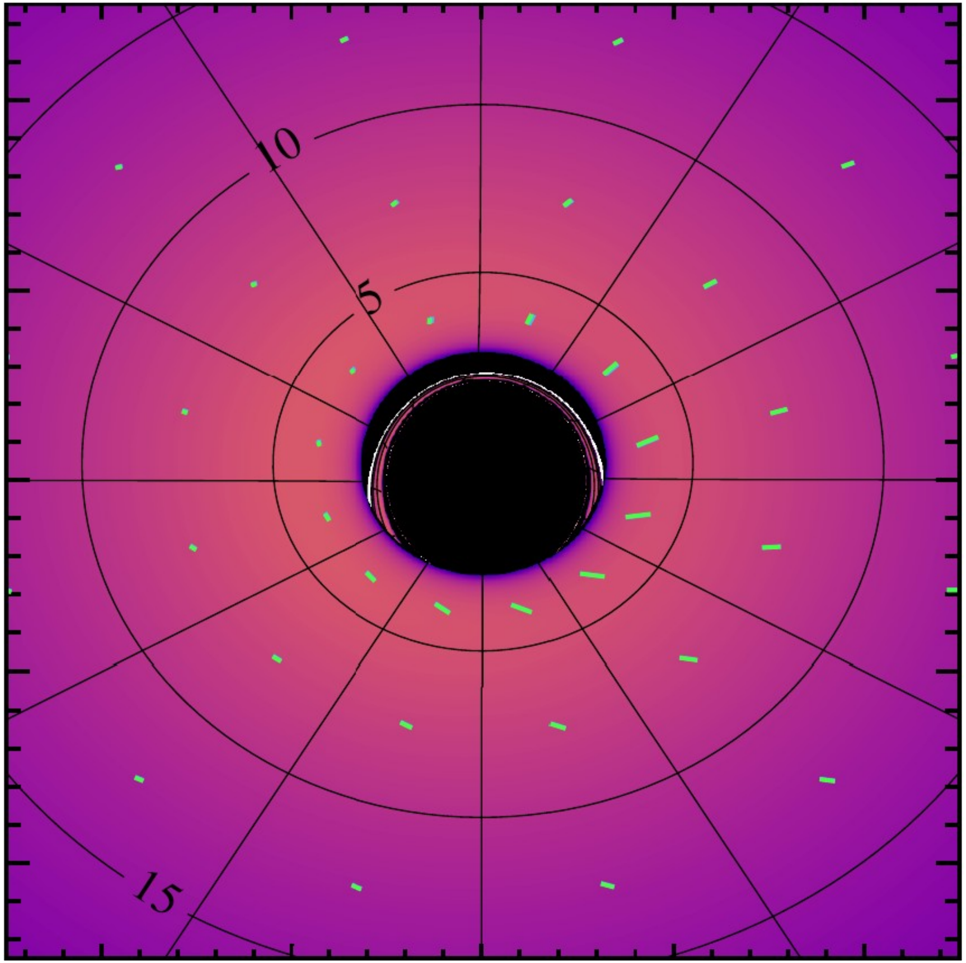

Model: Light bending (Schwarzschild)

- The trajectories in the Schwarzschild metric are **planar**
- We do not compute the full trajectory but **explicitly** define the emission angle at the disk.
- We have **analytical** expressions and very good one-line approximation of the light bending
- The PA rotation is also expressed analytically (fast)

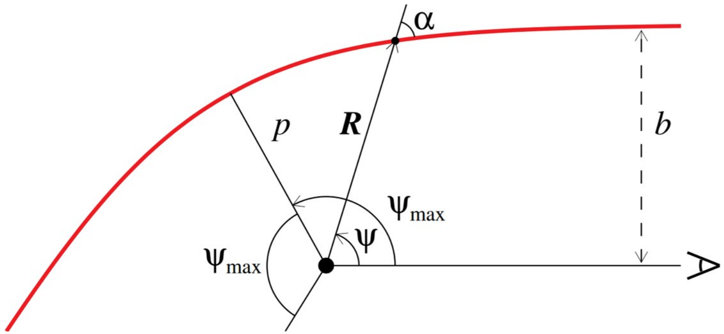

$$\psi(R,\alpha) = \int_R^{\infty} \frac{\mathrm{d}r}{r^2}\left[\frac{1}{b^2} - \frac{1}{r^2}\left(1 - \frac{R_S}{r}\right)\right]^{-1/2}$$

$$x = (1-u)y\left(1 + \frac{u^2y^2}{112} - \frac{e}{100}uy(\ln(1-y/2) + y/2)\right),$$

where $x = 1 - \cos\alpha$, $y = 1 - \cos\psi$, and $u = 2/r$.

[Poutanen, J. 2020]

Comparing our method with the numerical ray-tracing

*using ARCMANCER [Pihajoki et. al. 2018]

Comparison: at ISCO

- PA rotation (χ^{tot}) and local emission angle (ζ') as a function of azimuth at the ISCO for different BH spins and iclinations.
- The spin are a = 0.2, 0.5, 0.8
- Inclinations are **30°**, **60°**, **80°.**
- The discrepancy between the methods is only significant for the light coming from the disk behind the BH, where the features are shifted by the Kerr frame-dragging

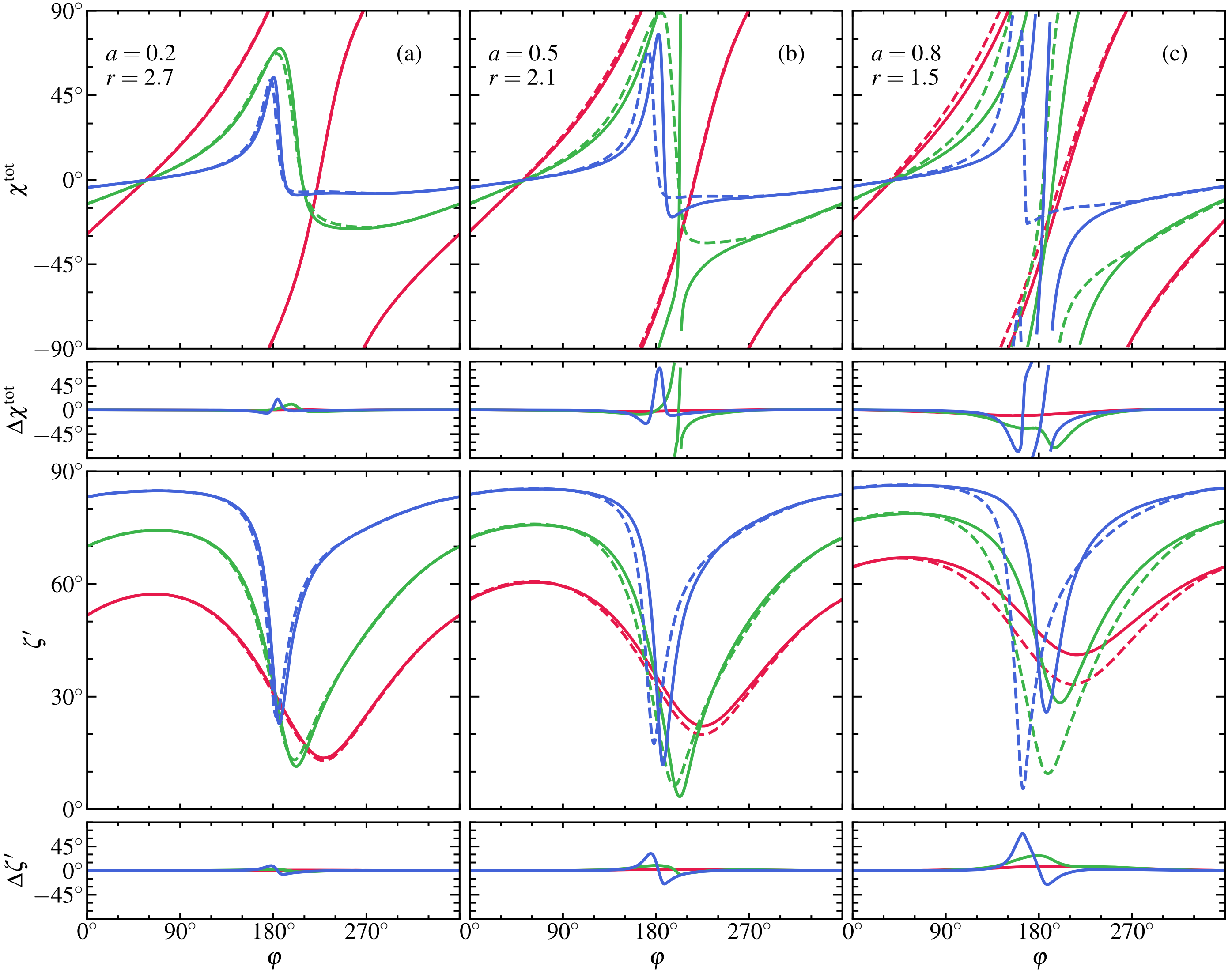

Comparison: wider rings

- PA rotation (χ^{tot}) and local emission angle (ζ’) as a function of azimuth at different distances from the BH
- The spin is 0.8,
- At r = $2R_S$, $3R_S$, $5R_S$
- Inclinations are **30°**, **60°**, **80°.**
- The difference is even less pronounced the further the emitting spot is from the BH

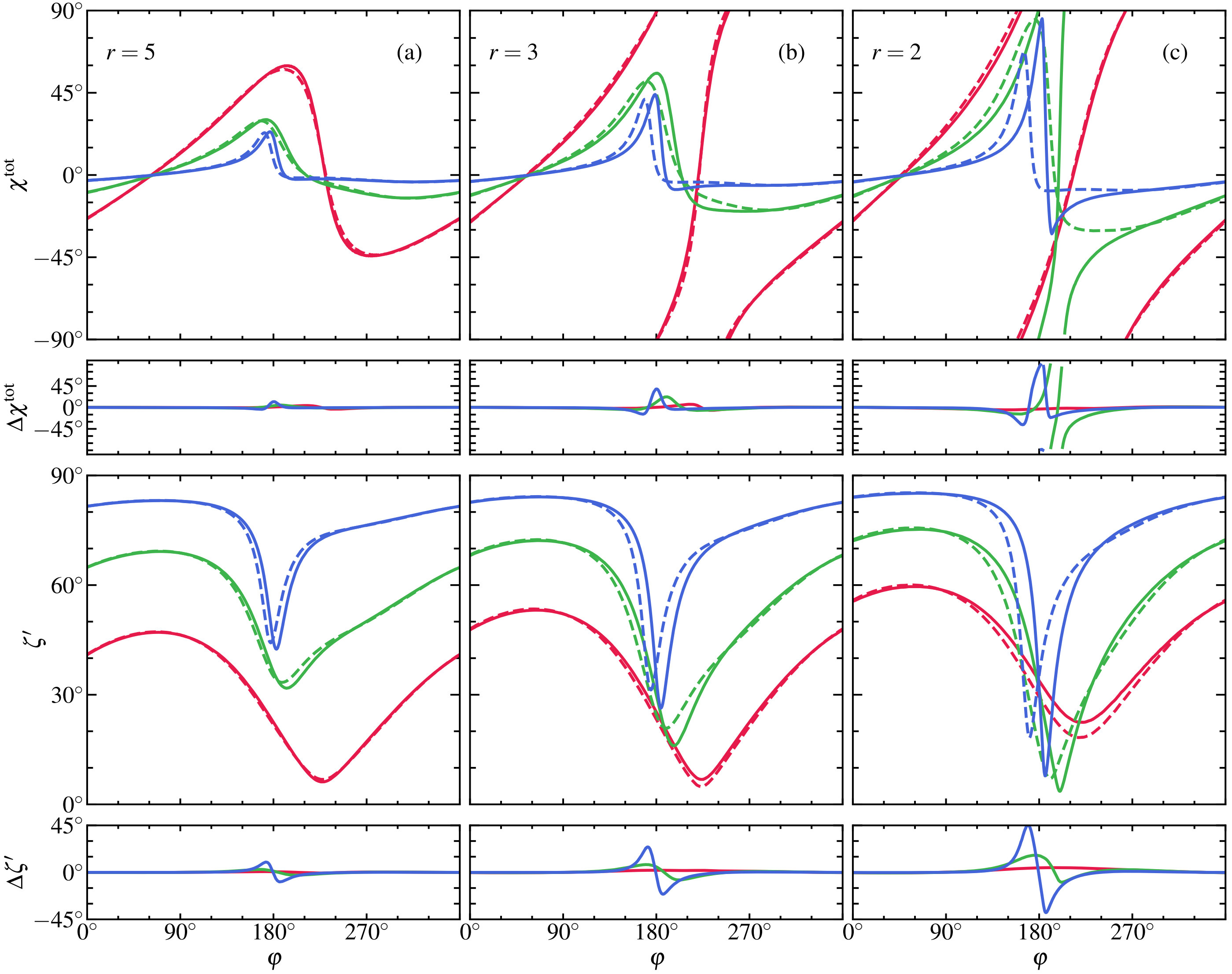

Comparison: imaging

- Images of a thin disk, the inner part **< 12 R$_s$**
- The spins are a = **0.2, 0.5, 0.8** left to right
- Inclinations are **30°**, **60°**, **80°** top to bottom
- The sticks show polarization computed with **analytical** and **numerical** method, and colormap shows the relative intensity.
- Unless lower right corner, the difference is hard to see.

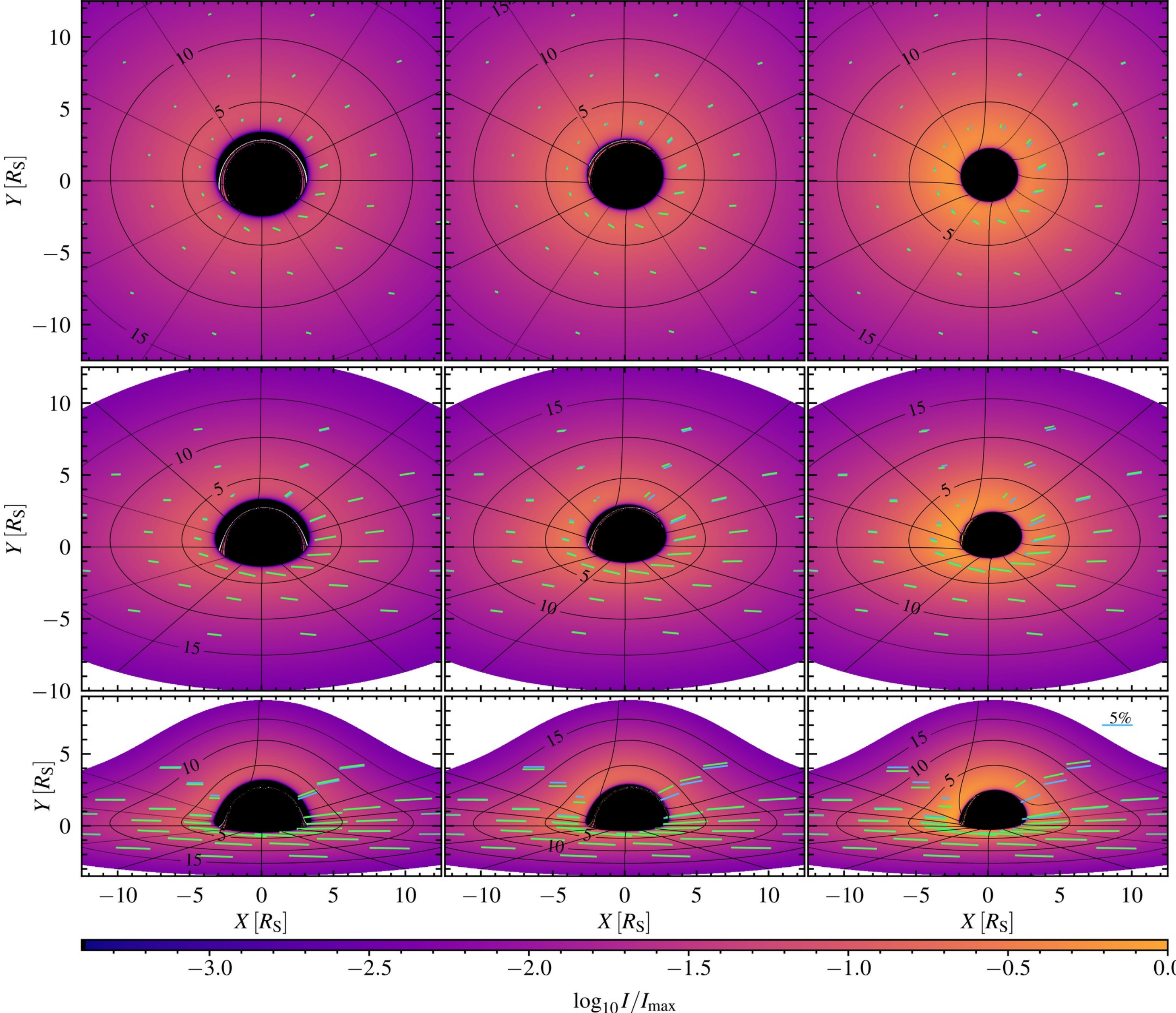

Comparison: spectra

- Polarizaton spectra: relative luminocity (top), PD (middle) and PA (bottom)
- Numerical (dashed) versus analytical (solid)
- The spins are a = **-1**, **0**, **0.5**, **0.8**, **0.94**
- Inclinations are **30°**, **60°**, **80°** left to right.
- For small inclinations th difference is very small.
- For **a > 0.94** the ISCO is below R_S
- In general for **a < 0.8** the results are quite adequate.

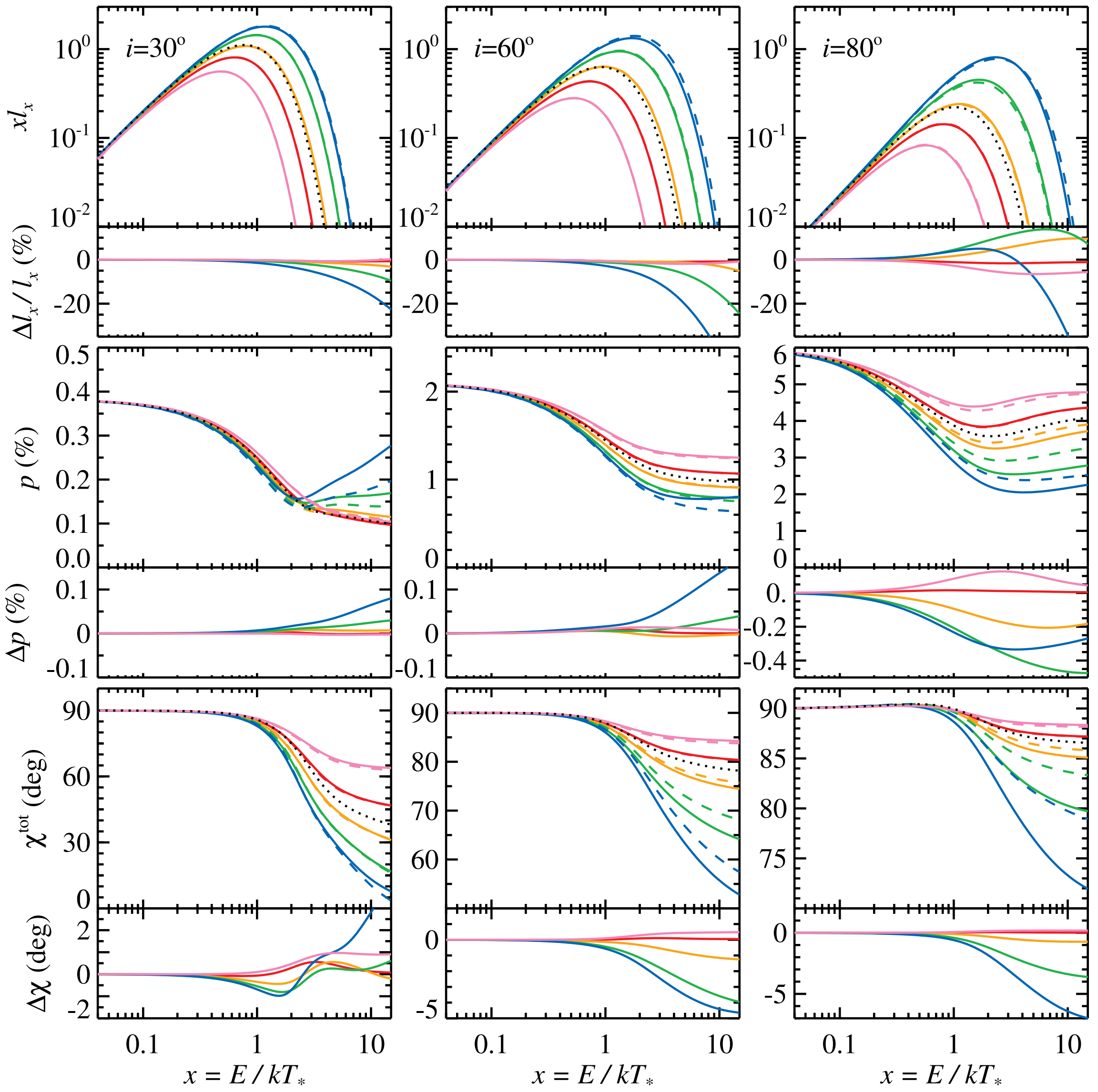

Conclusions

- We developed a fast method of computing polarization spectra from Kerr BH XRBs leveraging the Schwarzschild approximatoin of the light bending
- We tested our method against exact numerical ray-tracing techniques
- The results are accurate for inclinations **< 80°** or spins **< 0.8**
- Our method allows fast and flexible computation of polarization spectra.
- Our method is used to analyse the IXPE observations such as of CygX-1

Conclusions

- We developed a fast method of computing polarization spectra from Kerr BH XRBs leveraging the Schwarzschild approximatoin of the light bending
- We tested our method against exact numerical ray-tracing techniques
- The results are accurate for inclinations **< 80°** or spins **< 0.8**
- Our method allows fast and flexible computation of polarization spectra.
- Our method is used to analyse the IXPE observations such as of CygX-1

Thank you

Contribution of the secondary images

Contribution is less than 0.5% across all cases